www.icgst.com

Employing Vector Multiplication and Tilt Compensation Algorithm in Mimicking a Three Degree of Freedom Robotic Shoulder

J. Abliter, E. Agustin, M. Arroyo, A. Morante, J. Taduran, R. Tolentino
Electronics Engineering - Polytechnic University of the Philippines (Santa Rosa Campus)
Tagapo, Santa Rosa City, Laguna
johnmarkabliter@ymail.com, eugenenitsuga04@gmail.com, maerikaannearroyo@gmail.com,
mandreaalette@gmail.com, taduranjayson@ymail.com, kenmetara@yahoo.com
https://www.pup.edu.ph/

Abstract
The study aims to apply tri-axial accelerometers and magnetometer for acquiring angle in mimicking robotic shoulder using Vector Multiplication and Tilt Compensation Algorithm. The accelerometers and magnetometer are the main sensors where in the accelerometers are attached to the spine, right shoulder, upper arm and lower arm in slanting position of the user to acquire the pitch and roll movement. The magnetometer-accelerometer pair is attached on the top of the shoulder joint to acquire the yaw movement. The authors apply the concept of Vector Multiplication and Tilt Compensation Algorithm in the computation to obtain the angle of the human shoulder. The authors use C programming and LabVIEW Robotics software for extraction of the data to be used. Furthermore, the authors assert that the system is effective in acquiring the user's shoulder angle for mimicking robotic shoulder. Similarly, the authors analyze that the user's actual shoulder angle is close to the robotic shoulder prototype angle.

Keywords: *Accelerometers, Magnetometer, Shoulder Angle, Robotic Shoulder, Vector Multiplication, Tilt Compensation Algorithm*

Nomenclature

DOF	Degree-of-Freedom
IDE	Integrated Development Environment
NI VISA	National Instruments Virtual Instrument Software Architecture

1. Introduction
In the recent years, the development of interaction between robots and humans has become a key research topic in the field of robotics. Mimicking robotics is one of the important applications in the vast field of robotics, whereas the robots are being controlled by specific movements. Methods and techniques had been developed and different sensors have been used to capture human motion to manipulate the movements of the robot [1]. A lot of robots today use high cost integrated force torque sensors and cameras in order to detect human motion. However, the most common and cheapest of these sensors are the accelerometers and magnetometers. Accelerometers can determine the position and orientation of an object. It is used to sense not only the gravity (tilt) but the sudden acceleration within a certain range of motion [2]. However, it had certain disadvantages like acquiring slow responses, being sensitive to acceleration forces due to movement and not knowing lateral orientation (yaw) because it only has a vertical reference (gravity) but not horizontal reference. On the other hand, magnetometers measure direction and strength of magnetic field along one dimension. It can be used to detect earth's magnetic field, which always points to north. This reference contains the horizontal component, from which it is possible to read off lateral orientation of the device, unlike accelerometers [3]. Combining these two sensors, it was possible to acquire angles that can be used to mimic human motion.

Various groups had attempted to create solutions in acquiring angles for mimicking human motion. Such works include a research work which attempted to create solutions to accurately translate human motions using Kinect Sensor by applying Vector Multiplication Approach such as Euclidean Distance, Cross Product, and Dot Product Approach [4]. Another work had determined the angular position of the elbow joint by attaching two tri-axial accelerometers to the upper arm and forearm of the user. The data obtained from the accelerometers were used to control the robotic elbow. [5] Another study combined kinematic models designed for control of robotic arms with state space methods to estimate angles of the human shoulder and elbow using gyroscope and accelerometer. The algorithm was tested on a 6-DOF (Degree of Freedom) industrial robotic arm wherein the shoulder joint was limited to only 2-DOF (pitch and yaw) movement [6]. The problem was that it only acquired the pitch and yaw angles of the human shoulder movement. If these acquired angles will be used to mimic the human shoulder movement, it will be inaccurate because the human shoulder requires 3-DOF which are the pitch, roll, and yaw movement.

In this paper, the main objective was to apply accelerometers to mimic the 2-DOF (pitch and roll) movement of the human shoulder using Vector Multiplication. The study can help the industry, in the manufacturing process. In this 3-DOF shoulder, the addition of 1-DOF also increases the robot's reach which means that the range of movement in each of its joints is considerably greater. This study can also help the medical field, in physical therapy and rehabilitation. The project is intended to aid in diagnosis of movement disorders. The magnetometer and accelerometer sensors are applied to mimic the remaining 1-DOF (yaw) movement of the human shoulder using Tilt Compensation Algorithm. The accelerometers are attached to the spine, upper arm, lower arm, and right shoulder of the user. The magnetometer-accelerometer pair is placed at the top of the shoulder joint. The robotic shoulder will move as the sensors measure the shoulder angles. The digital outputs of the sensors are read by the Arduino using LabVIEW Robotics which uses different mathematical approach to calculate the shoulder joint angles. This data is then feed to the servomotors by the Arduino using serial communication, for it to actuate the computed angles. Several tests are done to evaluate the proposed system. The results of the performed tests are presented and discussed.

2. Theory

The system is composed of a 3-DOF robotic shoulder equipped with Arduino Mega microcontroller, and actuated by three servo motors mounted at the robotic shoulder. Also, it is composed of a wearable device with the sensors. Another wearable device serves as measuring device comprised of potentiometer mounted on a 3-DOF mechanical joint that is used to know the actual shoulder angle produced by the user. Lastly, it is also composed of a computer running the program.

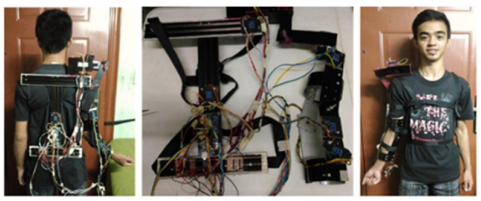

(a)

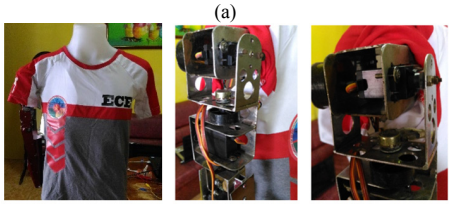

(b)

Figure 1. Wearable Device (a) and Robotic Shoulder (b)

The accelerometer and magnetometer in this study are the ADXL345 digital accelerometer and HMC5883L magnetometer. The communication between the sensors and the computer are coded in Arduno IDE (Integrated Development Environment). Figure 2 shows the explanation of how the system works. The authors used Arduino and LabVIEW software for the interfacing of program.

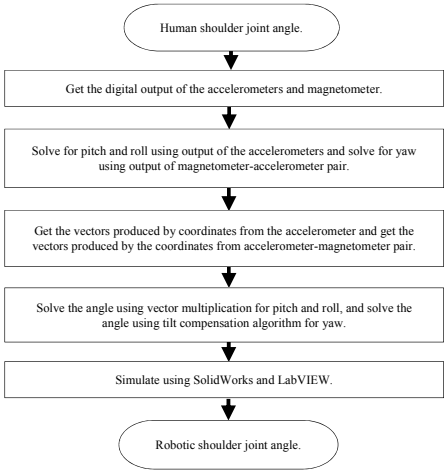

Figure 2. Conceptual Framework

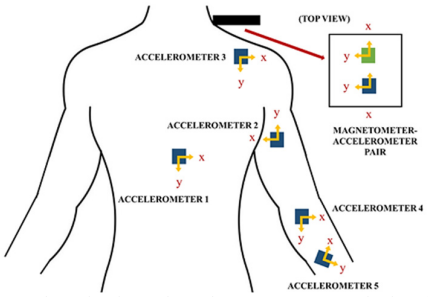

Figure 3. Selected points where the sensors are attached to the user

1. Steps in Acquiring Pitch and Roll Angle

The accelerometer has digital output in the range from -256 to +256 through 180° of tilt. The output in every axis (x-, y- and z-axis) is minimum if the axis is pointing downward, on the other hand, it has maximum value if it is pointing upward. The authors used these outputs to compute the acceleration due to gravity in different axes of the accelerometer which are attached to the user in the following selected points.

To the spine:

$$G'x_1 = \frac{-DOx_1}{s} \qquad Gy_1 = \frac{DOy_1}{s} \qquad Gz_1 = \frac{DOz_1}{s} \tag{1}$$

Where:
DO_{X1} = digital output from the X-axis of the accelerometer
DO_{Y1} = digital output from the Y-axis of the accelerometer
DO_{Z1} = digital output from the Z-axis of the accelerometer
S = the sensitivity of the accelerometer
G'_{X1} = acceleration from the X-axis of the accelerometer
G_{Y1} = acceleration from the Y-axis of the accelerometer
G_{Z1} = acceleration from the Z-axis of the accelerometer

To the upper arm:

$$Gx_2 = \frac{DOx_2}{s} \qquad G'y_2 = \frac{-DOy_2}{s} \qquad Gz_2 = \frac{DOz_2}{s} \tag{2}$$

To the right shoulder:

$$G'x_3 = \frac{-DOx_3}{s} \qquad Gy_3 = \frac{DOy_3}{s} \qquad Gz_3 = \frac{DOz_3}{s} \tag{3}$$

To the lower arm:

$$G'x_4 = \frac{-DOx_4}{s} \qquad Gy_4 = \frac{DOy_4}{s} \qquad Gz_4 = \frac{DOz_4}{s} \tag{4}$$

To the lower arm in slanting position:

$$G'x_5 = \frac{-DOx_5}{s} \qquad Gy_5 = \frac{DOy_5}{s} \qquad Gz_5 = \frac{DOz_5}{s} \tag{5}$$

By using the value of acceleration due to gravity in different axes of the accelerometers, the authors compute the value of tilt angles which are static measurement of accelerometers by performing the definition of tangent function. These tilt angles are named as roll and pitch angles. To determine the value of pitch angles of the accelerometers, the proponents get the angle formed by the accelerometer with respect to vertical axis.

$$\phi_1 = \tan^{-1}\left(\frac{Gy_1}{G'x_1}\right) \tag{6}$$

$$\phi_2 = \tan^{-1}\left(\frac{G'y_2}{Gx_2}\right) \tag{7}$$

$$\phi_3 = \tan^{-1}\left(\frac{-Gy_3}{G'x_3}\right) \tag{8}$$

$$\phi_4 = \tan^{-1}\left(\frac{Gy_4}{G'x_4}\right) \tag{9}$$

$$\phi_5 = \tan^{-1}\left(\frac{Gy_5}{G'x_5}\right) \tag{10}$$

Where:
ϕ_1 = pitch angle of the accelerometer (spine)
ϕ_2 = pitch angle of the accelerometer (upper arm)
ϕ_3 = pitch angle of the accelerometer (right shoulder)
ϕ_4 = pitch angle of the accelerometer (lower arm)
ϕ_5 = pitch angle of the accelerometer (lower arm in slanting position)

To determine the value of and roll angles of the accelerometer the authors used the following formulas:

$$\theta_1 = \tan^{-1}\left(\frac{Gz_1}{\sqrt{(G'x_1)^2 + (Gy_1)^2}}\right) \tag{11}$$

$$\theta_2 = \tan^{-1}\left(\frac{Gz_2}{\sqrt{(Gx_2)^2 + (G'y_2)^2}}\right) \tag{12}$$

$$\theta_3 = \tan^{-1}\left(\frac{Gz_3}{\sqrt{(G'x_3)^2 + (-Gy_3)^2}}\right) \tag{13}$$

$$\theta_4 = \tan^{-1}\left(\frac{Gz_4}{\sqrt{(G'x_4)^2 + (Gy_4)^2}}\right) \tag{14}$$

$$\theta_5 = \tan^{-1}\left(\frac{Gz_5}{\sqrt{(G'x_5)^2 + (Gy_5)^2}}\right) \tag{15}$$

Where:
θ_1 = roll angle of the accelerometer (spine)
θ_2 = roll angle of the accelerometer (upper arm)
θ_3 = roll angle of the accelerometer (right shoulder)
θ_4 = roll angle of the accelerometer (lower arm)
θ_5 = roll angle of the accelerometer (lower arm in slanting position)

These values are used to find the vector (radius) components of the spherical coordinates. From the orientation and position of accelerometers attached to the user, the value of roll and pitch angles correspond to the value of azimuth and zenith angle in spherical coordinates respectively. To determine the value of unit vectors (which are Vectors A, B, C, d and E) of the accelerometers, the authors used the following formulas:

$$\vec{A} = [(\sin\phi_1)(\cos\theta_1)]x + [(\sin\phi_1)(\sin\theta_1)]y + [(\cos\phi_1)]z \tag{16}$$

$$\vec{B} = [(\sin\phi_2)(\cos\theta_2)]x + [(\sin\phi_2)(\sin\theta_2)]y + [(\cos\phi_2)]z \tag{17}$$

$$\vec{C} = [(\sin\phi_3)(\cos\theta_3)]x + [(\sin\phi_3)(\sin\theta_3)]y + [(\cos\phi_3)]z \tag{18}$$

$$\vec{D} = [(\sin\phi_4)(\cos\theta_4)]x + [(\sin\phi_4)(\sin\theta_4)]y + [(\cos\phi_4)]z \tag{19}$$

$$\vec{E} = [(\sin\phi_5)(\cos\theta_5)]x + [(\sin\phi_5)(\sin\theta_5)]y + [(\cos\phi_5)]z \tag{20}$$

For the pitch, the accelerometers attached to the spine and upper arm are used by connecting the selected joint coordinates, a vector will be formed. The magnitude of each of the vector produced by joint coordinates must be known to be able to calculate the pitch and roll angle. For the pitch, these vectors are named as Vector A and Vector B for the imaginary lines from the spine to center shoulder and right shoulder to elbow, respectively.

The accelerometers attached to the right shoulder, upper arm and lower arm in slanting position are used for the roll movement. The vectors are named as Vector B, Vector C and Vector E for the imaginary lines from the derived point in the third accelerometer to right shoulder and derived point in the second accelerometer to right elbow, respectively.

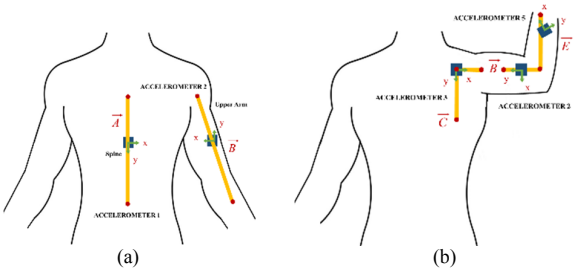

(a) (b)

Figure 4. Construction of Vectors for (a) Pitch and (b) Roll

With the use of Vector Multiplication, the angle of the pitch and roll can be calculated. For the pitch movement, the authors apply the Dot Product and for the roll movement both Dot and Cross Product are applied.

For the pitch movement, Vector A and B uses Dot Product to acquire the angle.

$$\angle P = \cos^{-1}\left(\frac{\vec{A} \bullet \vec{B}}{\left|\vec{A}\right|\left|\vec{B}\right|}\right) \tag{21}$$

$$\angle P = \cos^{-1}\frac{\left\{\begin{array}{l}\left[(\sin\phi_1)(\cos\theta_1)(\sin\phi_2)(\cos\theta_2)\right] + \\ \left[(\sin\phi_1)(\sin\theta_1)(\sin\phi_2)(\sin\theta_2)\right] + \\ \left[(\cos\phi_1)(\cos\phi_2)\right]\end{array}\right\}}{\left\{\begin{array}{l}\left[\sqrt{(\sin\phi_1\cos\theta_1)^2 + (\sin\phi_1\sin\theta_1)^2 + (\cos\phi_1)^2}\right] \\ \left[\sqrt{(\sin\phi_2\cos\theta_2)^2 + (\sin\phi_2\sin\theta_2)^2 + (\cos\phi_2)^2}\right]\end{array}\right\}} \tag{22}$$

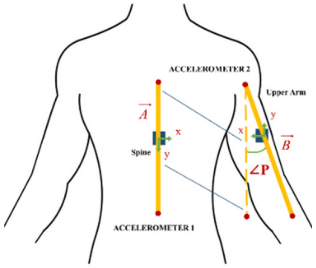

Figure 5. Calculation of Shoulder Angle for Pitch

For the roll movement, Vector F is calculated with the Cross Product of Vector C and B then, Vector G is calculated with the Cross Product of Vector E and the negative of Vector B. Then Dot Product is used in Vector F and G is used to acquire the roll angle. This is shown in the following formulas:

$$\vec{C} \times \vec{B} = \vec{F} = \begin{pmatrix} i & j & k \\ (\sin\phi_3)(\cos\theta_3) & (\sin\phi_3)(\sin\theta_3) & (\cos\phi_3) \\ (\sin\phi_2)(\cos\theta_2) & (\sin\phi_2)(\sin\theta_2) & (\cos\phi_2) \end{pmatrix} \tag{23}$$

$$\vec{F} = \left\{\begin{array}{l}\left[(\sin\phi_3)(\sin\theta_3)(\cos\phi_2) - (\sin\phi_2)(\sin\theta_2)(\cos\phi_3)\right]i + \\ \left[(\sin\phi_2)(\cos\theta_2)(\cos\phi_3) - (\sin\phi_3)(\cos\theta_3)(\cos\phi_2)\right]j + \\ \left[(\sin\phi_3)(\cos\theta_3)(\sin\phi_2)(\sin\theta_2) - (\sin\phi_2)(\cos\theta_2)(\sin\phi_3)(\sin\theta_3)\right]k\end{array}\right\} \tag{24}$$

$$\vec{E}\times-\vec{B}=\vec{G}=\begin{pmatrix} i & j & k \\ (\sin\phi_5)(\cos\theta_5) & (\sin\phi_5)(\sin\theta_5) & (\cos\phi_5) \\ -(\sin\phi_2)(\cos\theta_2) & -(\sin\phi_2)(\sin\theta_2) & -(\cos\phi_2) \end{pmatrix} \tag{25}$$

$$\vec{G}=\begin{Bmatrix} \left[-(\sin\phi_5)(\sin\theta_5)(\cos\phi_2)+(\sin\phi_2)(\sin\theta_2)(\cos\phi_5)\right]i+ \\ \left[-(\sin\phi_2)(\cos\theta_2)(\cos\phi_5)+(\sin\phi_5)(\cos\theta_5)(\cos\phi_2)\right]j+ \\ \left[-(\sin\phi_5)(\cos\theta_5)(\sin\phi_2)(\sin\theta_2)+(\sin\phi_2)(\cos\theta_2)(\sin\phi_5)(\sin\theta_5)\right]k \end{Bmatrix} \tag{26}$$

$$\angle R=\cos^{-1}\left(\frac{\vec{F}\bullet\vec{G}}{\left|\vec{F}\right|\left|\vec{G}\right|}\right) \tag{27}$$

$$\angle R=\cos^{-1}\frac{\begin{Bmatrix}\left[(\sin\phi_3)(\sin\theta_3)(\cos\phi_2)-(\sin\phi_2)(\sin\theta_2)(\cos\phi_3)\right] \\ \left[-(\sin\phi_5)(\sin\theta_2)(\cos\phi_2)+(\sin\phi_2)(\sin\theta_2)(\cos\phi_5)\right]\end{Bmatrix}+\begin{Bmatrix}\left[(\sin\phi_2)(\cos\theta_2)(\cos\phi_3)-(\sin\phi_3)(\cos\theta_3)(\cos\phi_2)\right] \\ \left[-(\sin\phi_2)(\cos\theta_2)(\cos\phi_5)+(\sin\phi_5)(\cos\theta_2)(\cos\phi_2)\right]\end{Bmatrix}+\begin{Bmatrix}\left[(\sin\phi_3)(\cos\theta_3)(\sin\phi_2)(\sin\theta_2)-(\sin\phi_2)(\cos\theta_2)(\sin\phi_3)(\sin\theta_3)\right] \\ \left[-(\sin\phi_2)(\cos\theta_5)(\sin\phi_2)(\sin\theta_2)+(\sin\phi_2)(\cos\theta_2)(\sin\phi_5)(\sin\theta_5)\right]\end{Bmatrix}}{\begin{Bmatrix}\left[(\sin\phi_3)(\sin\theta_3)(\cos\phi_2)-(\sin\phi_2)(\sin\theta_2)(\cos\phi_3)\right]^2+ \\ \left[(\sin\phi_2)(\cos\theta_2)(\cos\phi_3)-(\sin\phi_3)(\cos\theta_3)(\cos\phi_2)\right]^2+ \\ \left[(\sin\phi_3)(\cos\theta_3)(\sin\phi_2)(\sin\theta_2)-(\sin\phi_2)(\cos\theta_2)(\sin\phi_3)(\sin\theta_3)\right]^2\end{Bmatrix}^{\frac{1}{2}}\begin{Bmatrix}\left[-(\sin\phi_5)(\sin\theta_5)(\cos\phi_2)+(\sin\phi_2)(\sin\theta_2)(\cos\phi_5)\right]^2+ \\ \left[-(\sin\phi_2)(\cos\theta_2)(\cos\phi_5)+(\sin\phi_5)(\cos\theta_5)(\cos\phi_2)\right]^2+ \\ \left[-(\sin\phi_2)(\cos\theta_5)(\sin\phi_2)(\sin\theta_2)+(\sin\phi_2)(\cos\theta_2)(\sin\phi_5)(\sin\theta_5)\right]^2\end{Bmatrix}^{\frac{1}{2}}} \tag{28}$$

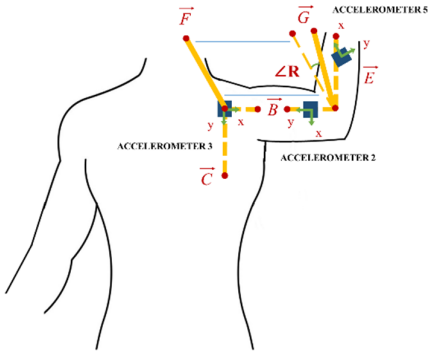

Figure 6. Calculation of Shoulder Angle for Roll

2. Steps in Acquiring Yaw Angle

The magnetometer-accelerometer pair is attached to the shoulder joint to mimic the yaw movement of the human shoulder. The magnetometer axes are the vectors acquired which is equal to the following:

$$MAG_{x-axis}=(DO_{MAGx-axis})(R_{MAG}) \tag{29}$$

Where:

$DO_{MAGx\text{-}axis}$ = digital output from the X-axis of the magnetometer in the shoulder joint

R_{MAG} = the resolution of the magnetometer

$MAG_{x\text{-}axis}$ = vector from the X-axis of the magnetometer in the shoulder joint

$$MAG_{y-axis}=(DO_{MAGy-axis})(R_{MAG}) \tag{30}$$

$$MAG_{z-axis}=(DO_{MAGz-axis})(R_{MAG}) \tag{31}$$

After getting the magnetometer axes, the authors also acquired the normalized X-axis and Y-axis of the accelerometer attached to the shoulder joint of the user which is equal to the following:

$$N_{x-axis}=(DO_{ACCx-axis})(R_{ACC})(gf) \tag{32}$$

Where:

$DO_{ACCx\text{-}axis}$ = digital output from the X-axis of the accelerometer in the shoulder joint

R_{ACC} = the resolution of the accelerometer

gf = gravity factor

$N_{x\text{-}axis}$ = normalized X-axis of the accelerometer in the shoulder joint

$$N_{y-axis}=(DO_{ACCy-axis})(R_{ACC})(gf) \tag{33}$$

By using the normalized axes, the authors computed the value of tilt angles which is the pitch and roll angle of the accelerometer.

$$\phi_6=\sin^{-1}(N_{y-axis}) \tag{34}$$

Where:

$N_{y\text{-}axis}$ = normalized Y-axis of the accelerometer in the shoulder joint

ϕ_6 = roll angle of the accelerometer (shoulder joint)

$$\theta_6=\sin^{-1}(N_{x-axis}) \tag{35}$$

Where:

$N_{x\text{-}axis}$ = normalized X-axis of the accelerometer in the shoulder joint

θ_6 = roll angle of the accelerometer (shoulder joint)

To determine the vectors to be used in the yaw movement of the shoulder, Tilt Compensation Algorithm is applied in order to acquire the X- and Y-axis of heading which are vectors in the magnetometer-accelerometer pair in the shoulder joint which is equal in the following:

$$X_h=(MAG_{x-axis})(\cos\phi_6)+(MAG_{z-axis})(\sin\phi_6) \tag{36}$$

Where:

$MAG_{x\text{-}axis}$ = vector from the X-axis of the magnetometer in the shoulder joint

$MAG_{z\text{-}axis}$ = vector from the Z-axis of the magnetometer in the shoulder joint

ϕ_6 = roll angle of the accelerometer (shoulder joint)

θ_6 = roll angle of the accelerometer (shoulder joint)

X_h = X-axis of heading

$$Y_h=\begin{Bmatrix}(MAG_{x-axis})(\sin\phi_6)(\sin\theta_6)+(MAG_{y-axis})(\cos\theta_6) \\ -(MAG_{z-axis})(\cos\phi_6)(\sin\theta_6)\end{Bmatrix} \tag{37}$$

In acquiring the yaw movement properly and accurately, it is necessary to take into account the error factor: the magnetic declination. Magnetic declination is the angle on the horizontal plane between magnetic north (the direction the north end of a compass needle points, corresponding to the direction of the Earth's magnetic field lines) and true north (the direction along a meridian towards the geographic North Pole). This angle varies depending on the position on the Earth's surface, and changes over time (year). The value of the current magnetic declination can be found on the special magnetic maps, as well as navigation maps. The authors used a magnetic declination of 2°2' W (negative) based on the current location of the user. To convert the angle into radians, the authors used the following formula:

$$MagneticDeclinationAngle=\frac{\deg ree+\frac{\min ute}{60}}{\frac{180}{\pi}} \tag{38}$$

To obtain the yaw movement, the proponents used the formula below:

$$\angle Y=\tan^{-1}\left(\frac{Y_h}{X_h}\right)\pm MagneticDeclinationAngle \tag{39}$$

To correct the yaw angle from 0° to 360°:

$$if \angle Y < 0$$
$$CorrectYawAngle = \angle Y + 2\pi$$
$$if \angle Y > 0$$
$$CorrectYawAngle = \angle Y - 2\pi$$

To correct the rotation of the yaw angle, subtract the correct yaw angle from 360°:

$$\angle Y = 360^{\circ} - CorrectYawAngle(\frac{180^{\circ}}{\pi}) \quad (40)$$

3. Evaluation of the System

The authors devised a wearable device comprised of three potentiometers for each movement which is mounted on a 3-DOF mechanical joint. The proponents used the data coming from the accelerometers to acquire the shoulder angle by applying the mathematical methods discussed. The computed angle is read by the Arduino microcontroller. The authors also used potentiometer in the wearable sensor to compare data from the sensors. For the acquisition of prototype shoulder angle for pitch, roll and yaw, the authors devised a potentiometer-mounted robotic shoulder to translate its mechanical movement into analog signal.

Figure 7. Acquisition of Robotic Shoulder Angle

The shoulder angle values are sent through serial communication into a PC and then, inputted into LabVIEW's waveform chart feature which plotted the graph to monitor the response using NI VISA. In controlling the robotic arm, the authors used servo motor as an actuator. The servo motor is connected to Arduino microcontroller and is attached to the joint of robotic shoulder. The movement of servo motor is dependent to the value of computed angle. To know the critical value for a two-tailed test, the significance level (α) is set to 5%. Setting this significance value will create a confidence of 95% (obtained by 100% - α), the area of the curve as the critical value is 0.975 (obtained by 1 – (α/2)). Knowing the area, the authors used the z-test table (area under the normal curve) and found the critical value 1.96. The authors will obtain the z value by using the z-test equation below:

$$z = \frac{\bar{X}_1 - \bar{X}_2}{\sqrt{\frac{(\sigma_1)^2}{n_1} + \frac{(\sigma_2)^2}{n_2}}} \quad (41)$$

Where:

z = z-test result
n_1 = no. of samples in the first group
n_2 = no. of samples in the second group
σ_1 = standard deviation of the first group
σ_2 = standard deviation of the second group
$\bar{x}_1$ = mean of the first group
$\bar{x}_2$ = mean of the second group

3. Results and Discussion

1. Acquisition of the Pitch and Roll Shoulder Angle

From the different angles made by the user, the authors obtained the data coming from the accelerometers. To analyze and interpret the computed angle, the authors gathered raw data through varying the movement of the human shoulder in random movements.

For Pitch: Table 1 and 2 shows the digital outputs in three different axes of accelerometers which are attached to the spine and upper arm, respectively. The accelerations due to gravity in every axis and the tilt angles are also shown. For Table 1, the vector is the orientation of the accelerometer in the spine with respect of the coronal plane of the user. For Table 2, the vector is the orientation of the accelerometer in the upper arm with respect to the arm of the user. From each angle the value of acceleration due to gravity in different axes and tilt angles are different from the other angles. It only shows that the user is moving from one angle to another.

Table 1. Data Obtained from the Accelerometer Attached to Spine

Accelerometer Attached to Spine								
Shoulder Angle (Pitch)	Digital Output of Accelerometer			Acceleration Due To Gravity			Tilt Angles	
	DOx1	DOy1	DOz1	Gx1	Gy1	Gz1	Φ1	θ1
20	-11	262	23	0.0430	1.0234	0.0898	87.5959	5.0125
30	-11	262	22	0.0430	1.0234	0.0859	87.5959	4.7956
40	-13	262	20	0.0508	1.0234	0.0781	87.1594	4.3599
50	-13	262	18	0.0508	1.0234	0.0703	87.1594	3.9254
60	-14	262	16	0.0547	1.0234	0.0625	86.9413	3.4897
70	-16	259	14	0.0625	1.0117	0.0547	86.4650	3.0882
80	-21	262	13	0.0820	1.0234	0.0508	85.4174	2.8315
90	-27	260	13	0.1055	1.0156	0.0508	84.0713	2.8471
100	-35	259	11	0.1367	1.0117	0.0430	82.3039	2.4101
110	-44	259	8	0.1719	1.0117	0.0313	80.3584	1.7442
120	-60	258	13	0.2344	1.0078	0.0508	76.9081	2.8097

Table 2. Data Obtained from the Accelerometer Attached to Upper Arm

Accelerometer Attached to the Upper Arm								
Shoulder Angle (Pitch)	Digital Output of Accelerometer			Acceleration Due To Gravity			Tilt Angles	
	DOx2	DOy2	DOz2	Gx2	Gy2	Gz2	Φ2	θ2
20	93	-227	3	0.3633	0.8867	0.0117	67.7215	0.7007
30	130	-208	4	0.5078	0.8125	0.0156	57.9946	0.9343
40	173	-189	6	0.6758	0.7383	0.0234	47.5308	1.3415
50	201	-152	18	0.7852	0.5938	0.0703	37.0973	4.0856
60	229	-115	21	0.8945	0.4492	0.0820	26.6650	4.6849
70	249	-75	20	0.9727	0.2930	0.0781	16.7626	4.3979
80	257	-25	18	1.0039	0.0977	0.0703	5.5560	3.9876
90	259	28	28	1.0117	-0.1094	0.1094	-6.1702	6.1347
100	248	81	43	0.9688	-0.3164	0.1680	-18.0877	9.3593
110	228	133	51	0.8906	-0.5195	0.1992	-30.2564	10.9356
120	193	184	46	0.7539	-0.7188	0.1797	-43.6325	9.7876

Table 3 shows the vector components of Vector A and B which are obtained from the accelerometers attached in the spine and the upper arm, the Scalar Product of the two vectors produced, the actual angle and computed shoulder angle, and their angle difference. The average of the angle difference obtained from this set of data was 0.2244° which is close to zero. It means that there is a small difference between the actual and computed shoulder angles. But still, the values of each computed pitch angle are close to the pitch shoulder angle of the user.

Table 3. Vector Components of the Accelerometers in the Spine and Upper Arm, the Scalar Product, the Comparison of Computed Shoulder Angle and Actual Shoulder Angle, and the Angle Difference for Pitch Movement

Shoulder Angle (Pitch)	A (Spine)			B (Upper Arm)			A · B	Computed Shoulder Angle	Angle Difference
	i	j	k	i	j	k			
20	0.9953	0.0873	0.0419	0.9253	0.0113	0.3791	0.9378	20.3108	0.3108
30	0.9956	0.0835	0.0419	0.8479	0.0138	0.5300	0.8676	29.8236	-0.1764
40	0.9959	0.0759	0.0496	0.7374	0.0173	0.6752	0.7692	39.7204	-0.2796
50	0.9964	0.0684	0.0496	0.6016	0.0430	0.7976	0.6420	50.0623	0.0623
60	0.9967	0.0608	0.0534	0.4473	0.0367	0.8936	0.4957	60.2827	0.2827
70	0.9966	0.0538	0.0617	0.2876	0.0221	0.9575	0.3468	69.7070	-0.2930
80	0.9956	0.0492	0.0799	0.0966	0.0067	0.9953	0.1760	79.8625	-0.1375
90	0.9934	0.0494	0.1033	-0.1069	-0.0115	0.9942	-0.0040	90.2314	0.2314
100	0.9901	0.0417	0.1339	-0.3063	-0.0505	0.9506	-0.1781	100.2600	0.2600
110	0.9854	0.0300	0.1675	-0.4947	-0.0956	0.8638	-0.3457	110.2249	0.2249
120	0.9728	0.0477	0.2265	-0.6800	-0.1173	0.7238	-0.5032	120.2100	0.2100
								Average Angle Difference	0.2244

For Roll: Table 4, 5 and 6 shows the digital outputs in three different axes of accelerometer attached to the right shoulder, lower arm in slanting position and upper arm, respectively. The accelerations due to gravity in every axis and the tilt angles are also shown.

Table 4. Data Obtained from the Accelerometer Attached to Right Shoulder

Accelerometer Attached to the Right Shoulder								
Shoulder Angle (Roll)	Digital Output of Accelerometer			Acceleration Due To Gravity			Tilt Angles	
	DOx3	DOy3	DOz3	Gx3	Gy3	Gz3	Φ3	θ3
0	-11	278	-1	0.0430	1.0859	-0.0039	87.7341	-0.2059
10	0	277	-7	0.0000	1.0820	-0.0273	90.0000	-1.4476
20	2	278	-10	-0.0078	1.0859	-0.0391	90.4122	-2.0601
30	-6	276	-12	0.0234	1.0781	-0.0469	88.7546	-2.4890
40	-8	277	-12	0.0313	1.0820	-0.0469	88.3457	-2.4795
50	-7	277	-14	0.0273	1.0820	-0.0547	88.5524	-2.8924
60	-6	278	-17	0.0234	1.0859	-0.0664	88.7636	-3.4985
70	-1	279	-13	0.0039	1.0898	-0.0508	89.7946	-2.6677
80	-5	276	-17	0.0195	1.0781	-0.0664	88.9621	-3.5241
90	-5	277	-20	0.0195	1.0820	-0.0781	88.9659	-4.1290
100	-6	275	-21	0.0234	1.0742	-0.0820	88.7501	-4.3658

Table 5. Data Obtained from the Accelerometer Attached to Lower Arm in Slanting Position

Accelerometer Attached to the Lower Arm in Slanting Position								
Shoulder Angle (Roll)	Digital Output of Accelerometer			Acceleration Due To Gravity			Tilt Angles	
	DOx5	DOy5	DOz5	Gx5	Gy5	Gz5	Φ5	θ5
0	206	-157	1	-0.8047	-0.6133	0.0039	-142.6877	0.2212
10	214	-153	-52	-0.8359	-0.5977	-0.2031	-144.4370	-11.1814
20	207	-144	-100	-0.8086	-0.5625	-0.3906	-145.1755	-21.6319
30	184	-134	-142	-0.7188	-0.5234	-0.5547	-143.9356	-31.9576
40	163	-114	-180	-0.6367	-0.4453	-0.7031	-145.0316	-42.1430
50	135	-87	-212	-0.5273	-0.3398	-0.8281	-147.2005	-52.8535
60	96	-64	-238	-0.3750	-0.2500	-0.9297	-146.3099	-64.1368
70	62	-51	-253	-0.2422	-0.1992	-0.9883	-140.5599	-72.3950
80	16	-24	-258	-0.0625	-0.0938	-1.0078	-123.6901	-83.6208
90	-25	1	-257	0.0977	0.0039	-1.0039	2.2906	-84.4395
100	-34	8	-259	0.1328	0.0313	-1.0117	13.2405	-82.3195

For Table 4, this vector is the orientation of the accelerometer in the right shoulder with respect to the coronal plane of the user. For Table 5, this vector is the orientation of the accelerometer in the lower arm in slanting position with respect to the arm of the user. And for Table 6, this vector is the orientation of the accelerometer in the upper arm with respect to the arm of the user. From each angle the value of acceleration due to gravity in different axes and tilt angles are different from the other angles. It only shows that the user is moving from one angle to another.

Table 6. Data Obtained from the Accelerometer Attached to Upper Arm

Accelerometer Attached to the Upper Arm								
Shoulder Angle (Pitch)	Digital Output of Accelerometer			Acceleration Due To Gravity			Tilt Angles	
	DOx2	DOy2	DOz2	Gx2	Gy2	Gz2	Φ2	θ2
0	255	-13	35	0.9961	0.0508	0.1367	2.9184	7.8053
10	255	-13	-15	0.9961	0.0508	-0.0586	2.9184	-3.3621
20	251	-14	-64	0.9805	0.0547	-0.2500	3.1925	-14.2832
30	227	-14	-98	0.8867	0.0547	-0.3828	3.5292	-23.3112
40	204	-2	-139	0.7969	0.0078	-0.5430	0.5617	-34.2682
50	172	3	-181	0.6719	-0.0117	-0.7070	-0.9992	-46.4561
60	128	4	-202	0.5000	-0.0156	-0.7891	-1.7899	-57.6264
70	95	-1	-220	0.3711	0.0039	-0.8594	0.6031	-66.6433
80	45	-1	-231	0.1758	0.0039	-0.9023	1.2730	-78.9739
90	1	-3	-232	0.0039	0.0117	-0.9063	71.5651	-89.2191
100	-14	-3	-233	-0.0547	0.0117	-0.9102	167.9052	-86.4836

Table 7 shows the vector components of Vector B, Vector C and Vector E which are obtained from the accelerometers attached in the upper arm, lower arm in slanting position and the right shoulder.

Table 7. Vector Components of the Accelerometers in the Upper Arm, Lower Arm in Slanting Position and Right Shoulder for Roll Movement

Shoulder Angle (Roll)	B (Upper Arm)			C (Right Shoulder)			E (Lower Arm)		
	i	j	k	i	j	k	i	j	k
0	0.0504	0.0069	0.9987	0.9992	-0.0036	0.0395	-0.6062	-0.0023	-0.7953
10	0.0508	-0.0030	0.9987	0.9997	-0.0253	0.0000	-0.5706	0.1128	-0.8135
20	0.0540	-0.0137	0.9984	0.9993	-0.0359	-0.0072	-0.5308	0.2105	-0.8209
30	0.0565	-0.0244	0.9981	0.9988	-0.0434	0.0217	-0.4995	0.3116	-0.8084
40	0.0081	-0.0055	1.0000	0.9986	-0.0432	0.0289	-0.4250	0.3846	-0.8195
50	-0.0120	0.0126	0.9998	0.9984	-0.0504	0.0253	-0.3271	0.4318	-0.8406
60	-0.0167	0.0264	0.9995	0.9979	-0.0610	0.0216	-0.2420	0.4991	-0.8321
70	0.0042	-0.0097	0.9999	0.9989	-0.0465	0.0036	-0.1921	0.6055	-0.7723
80	0.0042	-0.0218	0.9998	0.9979	-0.0615	0.0181	-0.0924	0.8269	-0.5547
90	0.0129	-0.9486	0.3162	0.9972	-0.0720	0.0180	0.0039	-0.0398	0.9992
100	0.0129	-0.2091	-0.9778	0.9969	-0.0761	0.0218	0.0306	-0.2270	0.9734

Table 8 shows the vector components of the cross product of Vector C and B which is equal to Vector F and the vector components of the cross product of Vector E and Vector -B which is equal to Vector G. Table 8 also shows the magnitudes of Vector F and Vector G and its Dot Product.

Table 8. Vector Components from the Cross Product and Dot Product Using Vectors B, C and E, for Roll Movement

Shoulder Angle (Roll)	F = C x B			G= E x -B			F	G	F · G
	i	j	k	i	j	k			
0	-0.0039	-0.9959	0.0071	-0.0032	-0.5652	0.0041	0.9960	0.5653	0.5630
10	-0.0252	-0.9984	-0.0017	-0.1102	-0.5285	0.0040	0.9987	0.5399	0.5392
20	-0.0360	-0.9982	-0.0118	-0.1989	-0.4857	0.0041	0.9989	0.5249	0.5243
30	-0.0428	-0.9957	-0.0219	-0.2913	-0.4528	0.0054	0.9969	0.5385	0.5368
40	-0.0431	-0.9984	-0.0052	-0.3800	-0.4183	0.0008	0.9993	0.5651	0.5647
50	-0.0508	-0.9986	0.0120	-0.4423	-0.3372	-0.0011	0.9999	0.5562	0.5561
60	-0.0615	-0.9978	0.0253	-0.5208	-0.2558	-0.0020	1.0000	0.5803	0.5803
70	-0.0465	-0.9988	-0.0095	-0.5980	-0.1889	0.0007	1.0000	0.6271	0.6271
80	-0.0610	-0.9976	-0.0215	-0.8146	-0.0901	0.0015	0.9997	0.8196	0.8193
90	-0.0056	-0.3151	-0.9450	-0.9353	-0.0117	0.0032	0.9962	0.9353	0.9318
100	0.0790	0.9750	-0.2075	-0.4255	-0.0424	0.0035	1.0000	0.4276	0.4276

Table 9 shows the comparison of the actual angle and the computed shoulder angle and the angle difference between them. The average of the angle difference obtained is 0.2496° which is close to zero. It means that there is a small difference between the actual and computed shoulder angles. But still, the values of each computed pitch angle are close to the pitch shoulder angle of the user.

Table 9. Comparison of the Actual Shoulder Angle, Computed Shoulder Angle and Angle Difference for Roll Movement

Shoulder Angle (Roll)	Actual Shoulder Angle	Computed Shoulder Angle	Angle Difference
0	0	0.0986	0.0986
10	10	10.3451	0.3451
20	20	20.2360	0.2360
30	30	30.3458	0.3458
40	40	39.7852	-0.2148
50	50	49.7807	-0.2193
60	60	60.3323	0.3323
70	70	69.8052	-0.1948
80	80	80.1935	0.1935
90	90	89.6323	-0.3677
100	100	100.1977	0.1977
	Average Angle Difference		0.2496

2. Acquisition of the Yaw Shoulder Angle

From the different angles made by the user, the authors obtained the data coming from the magnetometer-accelerometer pair. The table for digital outputs of magnetometer, normalized axes, tilt angles, x and y axis of heading, the computed and actual shoulder angle, and the total difference in each angle.

Table 10. Data Obtained from the Magnetometer-Accelerometer Pair Attached to the Shoulder Joint

Shoulder Angle (Yaw)	MAGX-axis	MAGY-axis	MAGZ-axis	nX-axis	nY-axis	Φ6	θ6	Xh	Yh
0	379.04	11.12	-139.84	-0.02	0	1.1460	0	376.1674	11.1200
10	384.48	-55.53	-140.76	0.02	-0.01	-1.1460	-0.5730	387.2183	-56.8576
20	382.50	-126.90	-140.76	0.01	0	-0.5730	0	383.8885	-126.9000
30	363.40	-195.96	-140.76	0.01	0	-0.5730	0	364.7894	-195.9600
40	330.44	-263.96	-142.60	0.03	0	-1.7191	0	334.5693	-263.9600
50	284.60	-322.92	-140.76	0.04	-0.02	-2.2924	-1.1460	290.0026	-325.4407
60	226.48	-365.24	-139.84	0.02	-0.03	-1.1460	-1.7191	229.2315	-369.1341
70	154.72	-397.44	-138.00	0.03	-0.02	-1.7191	-1.1460	158.7904	-400.0264
80	78.28	-412.16	-132.48	0.06	-0.02	-3.4398	-1.1460	86.0878	-414.6285
90	10.12	-411.24	-131.56	0.02	0.06	-1.1460	3.4398	12.7492	-402.6192

Table 10 shows the data obtained from the Magnetometer-Accelerometer Pair attached to the shoulder joint. The produced value of vector in magnetometer which are the $MAG_{X\text{-axis}}$, $MAG_{Y\text{-axis}}$ and the $MAG_{Z\text{-axis}}$, the normalized values of the axes of the accelerometer which are the $N_{X\text{-axis}}$ and $N_{Y\text{-axis}}$, the tilt angles, and the axes of headings which are X_h and Y_h of the magnetometer-accelerometer pair are shown in this table.

Table 11. Comparison of the Actual Shoulder Angle, Computed Shoulder Angle and Angle Difference for Yaw Movement

Shoulder Angle (Yaw)	Actual Shoulder Angle	Computed Shoulder Angle	Angle Difference
0	0	0.3401	0.3401
10	10	10.3867	0.3867
20	20	20.3254	0.3254
30	30	30.2774	0.2774
40	40	40.3052	0.3052
50	50	50.3289	0.3289
60	60	60.1931	0.1931
70	70	70.3827	0.3827
80	80	80.3039	0.3039
90	90	90.2196	0.2196
	Average Angle Difference		0.3063

Table 11 shows the comparison of the actual angle and the computed shoulder angle and the angle difference between them. The average of the angle difference obtained is 0.3063° which is close to zero. It means that there is a small difference between the actual and computed shoulder angles. But still, the values of each computed pitch angle are close to the pitch shoulder angle of the user.

3. Evaluation of the Significant Difference between Robotic Shoulder Angle Human Shoulder Angle

The user performs random movements to test the capability and the accuracy of the prototype to mimic its pitch, roll and yaw movements in different angles.

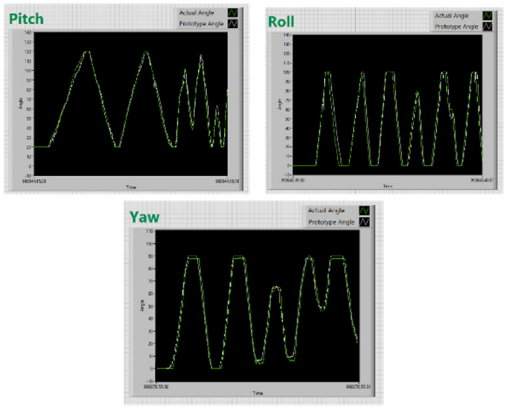

Figure 8. Lab VIEW Panel Showing the Graph of Actual and Prototype Angle for Pitch, Roll and Yaw Movement

The graph shows the actual and the prototype angle for the shoulder movements. The actual and the prototype angle for pitch, roll and yaw are always almost the same to each other. It is observed in the graph that the white line has more jitters than the green line, it simply indicates that the robotic shoulder has more noise than the actual shoulder. The noise and jitters are at minimum therefore, the response of the prototype to the user is realistic. Overall, it shows that the system has a good response in different shoulder movement. Below are the tables showing the pitch, roll and yaw movement for every angle and the results of z-test from the actual angle and robotic shoulder angle for pitch, roll and yaw.

Table 12, 13 and 14 shows the number of sample (n1 and n2), the mean of the sample ($\bar{x}1$ and $\bar{x}2$), the standard deviation of the sample (σ1 and σ2) and the z-test result. The results of the z-test for the pitch, roll and yaw shoulder movement are -0.2641, -0.3569 and -0.418, respectively. The results are close to zero. It means that the angular difference of actual angle and prototype angle is at minimum. It also means that the response is reliable. Therefore, the z-test result is in the acceptance region. Overall, there is no significant difference between the actual angle and the robotic shoulder angle for pitch, roll and yaw shoulder movement.

Table 12. Z-Test results for every Angle for Pitch Movement

Actual angle			Prototype angle			Result of Z-test	Comment
n1	$\bar{x}1$	σ1	n2	$\bar{x}2$	σ2		
600	66.9317	32.2157	600	67.4167	31.3973	-0.2641	Null Hypothesis is Accepted

Table 13. Z-Test results for every Angle for Roll Movement

Actual angle			Prototype angle			Result of Z-test	Comment
n1	$\bar{x}1$	σ1	n2	$\bar{x}2$	σ 2		
425	44.8424	34.0517	425	45.68	34.375	-0.3569	Null Hypothesis is Accepted

Table 14 Z-Test results for every Angle for Yaw Movement

Actual angle			Prototype angle			Result of Z-test	Comment
n_1	$\bar{x}_1$	σ_1	n_2	$\bar{x}_2$	σ_2		
410	46.6073	32.9803	410	47.5659	32.6761	-0.4181	Null Hypothesis is Accepted

4. Conclusion

The authors came with this findings based on the gathered data. The values of the acceleration due to gravity in different axis, pitch and roll angles obtained from the accelerometers varies in different angle, but it arrives with the angle close to the user's shoulder angle movement for pitch and roll movement. The average angle difference of the pitch, roll and yaw movement are close to zero which means that the method is effective for mimicking the shoulder's pitch and roll angle. This suggests that the system, the Vector Multiplication, Tilt Compensation Algorithm method proposed are effective in acquiring the value of user's pitch, roll and yaw shoulder angle. However, there is still slight angle difference between the actual shoulder angles and the computed shoulder angles due to unstableness of the accelerometer's tilt angles that easily affects the computed shoulder angles which can be seen in the inconsistency of the increasing and decreasing values of the tilt angles produced by each accelerometer. In terms of statistical data gathered by the authors, all of the z-test results for shoulder angles at different movement are within the range of -1.96 and +1.96, which means that the values are all accepted. Therefore, the prototype can effectively mimic the user's shoulder movements but it is also observed that there are some fluctuations of signal in the graphical response of the system. It is because of the noise and jitters caused by the system.

5. Recommendation

For future works, the authors recommend to use other methods that will minimize the effect of the unstableness of the accelerometer's tilt angles on the computed shoulder angles. It also suggests to use filtering methods on the system to lessen the jitter or noise that affects the response of the robotic shoulder. Thus, the future researchers may improve the response of the system.

6. References

[1] Ameri, Naghshineh and MazdakZereshki, "Human Motion Capture Using Tri-Axial Accelerometers", Institute of Electrical and Electronics Engineers Xplore (IEEE Xplore), 2009.

[2] Moreira, Pires and Pedro Neto, "Accelerometer Based Control of an Industrial Robotic Arm", Institute of Electrical and Electronics Engineers Xplore (IEEE Xplore), 2009.

[3] Madgwick, Sebastian, "Automated Calibration of Accelerometers, Magnetometers and Gyroscopes", Institute of Electrical and Electronics Engineers Xplore (IEEE Xplore), 2010.

[4] Emano, Mapalad, Siron, Ortega and Tolentino, "Vector Multiplication Approach for Point of View Variations in a Mimicking Robotic Shoulder Using Microsoft Kinect", International Journal of Inventive Engineering and Sciences (IJIES), Vol. 4, 2016.

[5] Alcira, Balla, Baris, Bilon, Burgos and Tolentino, "Scalar Product in Acquiring Angle for Mimicking Robotic Elbow using Two Tri-Axial Accelerometers", International Journal of Innovative Science and Modern Engineering (IJISME), Vol.4, 2016.

[6] El-Gohary, Mahmoud Ahmed, "Human Joint Angle Estimation with Inertial Sensors and Validation with a Robot Arm", Portland State University Dissertations and Theses, 2015.

Biographies

John Mark M. Abliter is currently studying the degree in Bachelor of Science in Electronics and Communications Engineering from the Polytechnic University of the Philippines Santa Rosa Campus, Laguna in 2017.

Eugene V. Agustin is currently studying the degree in Bachelor of Science in Electronics and Communications Engineering from the Polytechnic University of the Philippines Santa Rosa Campus, Laguna in 2017.

Ma. Erika Anne P. Arroyo is currently studying the degree in Bachelor of Science in Electronics and Communications Engineering from the Polytechnic University of the Philippines Santa Rosa Campus, Laguna in 2017.

Andrea Alette R. Morante is currently studying the degree in Bachelor of Science in Electronics and Communications Engineering from the Polytechnic University of the Philippines Santa Rosa Campus, Laguna in 2017.

Jayson C. Taduran is currently studying the degree in Bachelor of Science in Electronics and Communications Engineering from the Polytechnic University of the Philippines Santa Rosa Campus, Laguna in 2017.

Roselito E. Tolentino is a registered Electronics Engineer and IECEP-Member. He is a graduate of Bachelor of Science in Electronics and Communication Engineering at Adamson University in 2004. He finished his Master of Science in Electronics Engineering Major in Control System at Mapua Institute of Technology. He currently takes up Doctor of Philosophy in Electronics Engineering at the same Institute. He is currently working as a part time instructor at PUP - Santa Rosa Campus and DLSU-Dasmariñas.